PHYSICAL REVIEW A VOLUME 36, NUMBER 12 DECEMBER 15, 1987

Order-disorder transition in colloidal suspensions

R. O. Rosenberg and D. Thirumalai
Department of Chemistry and Biochemistry, and Institute for Physical Science and Technology, University of Maryland, College Park, Maryland 20742
(Received 15 June 1987)

The disorder-order transition observed in aqueous suspension of charged macroions is investigated with use of both simulations and a simple theoretical model. Molecular-dynamics (MD) simulations were performed by assuming that the interaction between the charge stabilized particles interact via a modified Debye-Hückel potential. The parameters of the potential were chosen to mimic the experimental study of Lindsay and Chaikin. Simulation results predict that the liquid freezes into a bcc phase in accord with the experimental findings. For comparison, the phase diagram with use of the self-consistent phonon theory (SCP) is presented. It is shown that the predictions of the SCP theory in the weak screening limit are in disagreement with both the MD results and the experiments. Possible reasons for this failure are pointed out. Finally, similar calculations have been carried out for the Yukawa potential. It is found that for the parameters considered here, this is an unphysical model for the suspensions of polystyrene spheres. No evidence for reentrant transitions is found in either of these models. This is in agreement with the predictions of the self-consistent phonon theory.

I. INTRODUCTION

Suspensions of highly charged particles, such as aqueous solutions of polystyrene spheres, can mimic the structural behavior found in more conventional liquids and solids.[1–4] It has been found the monodisperse charged polystyrene spheres[5,6] exhibit both liquidlike behavior and can crystallize[7] into a bcc or a fcc lattice under appropriate conditions of density and with the addition of added salt.[8–12] The crystalline structures, which can be thought of as classical Wigner crystals, have very large lattice spacings. The large lattice spacing (typically a few thousand angstroms) results in the elastic constants being about 10–12 orders of magnitude less than that of conventional solids.[9] These crystalline structures melt (undergo a first-order phase transition) when a suitable amount of salt is added, and in the limit of high concentration of the added salt, the structure of the colloidal liquid resembles that of a simple hard-sphere fluid system. Polydisperse suspensions of colloidal particles can result in the formation of exotic colloidal alloys and classical Wigner glasses.[9]

In this paper we consider the order-disorder transition in monodisperse aqueous suspensions of polystyrene spheres. The motivation for this study was provided by the recent experiments of Lindsay and Chaikin.[9] In addition, there does not appear to be any study of the first-order phase transition in charged colloids with the clarification of the role of interparticle interaction in determining the phase diagram. Many of the previous theoretical attempts have made use of an appropriate reference system to interpret the phenomena observed in suspensions. For example, the one-component Coulomb plasma has served as an appropriate reference system at low or zero electrolyte concentration[13–15] and the hard-sphere system has been used in the limit of strong screening.[16–21] Agreement between theory and experiment concerning the properties of the system (like the structure factor) is achieved by adjusting the one-component-plasma (OCP) coupling constant Γ or the hard-sphere diameter. Hone *et al.*[22] have used thermally-averaged lattice sums and have invoked the Lindemann law to predict melting parameters in colloidal suspensions. In a recent molecular dynamics simulation[23] it has been shown that this theory predicts qualitatively incorrect results raising the need for a more refined theoretical approach. Shih and Stroud[24] have modeled the liquid phase by a hard-sphere reference system. They determine the hard-sphere diameter and consequently the free energy of the liquid phase by utilizing the Gibbs-Bogolyubov inequality. The free energy of the solid phase was obtained using the classical harmonic approximation. They have also stressed the form of the interparticle interaction in determining reentrant melting in these systems.[24] The theory presented by Shih and Stroud does not appear to be successful in the screening regime corresponding to the experiments of Lindsay and Chaikin. A more detailed discussion of this point is made in Sec. IV.

In light of the empirical nature of the theories, we have performed molecular-dynamics simulations to determine the freezing and melting parameters in a model colloidal system. In addition these studies were undertaken to investigate the possibility of observing reentrant melting in charged stabilized systems. A self-consistent phonon theory is also presented and the phase diagram predicted by this theory is compared with the simulation results. These calculations were done using both the Einstein model and the Debye model for the oscillators. The present work also examines the consistency of empirical laws such as Verlet's rule and Lindemann criteria in determining freezing and melting pa-

rameters.

A recent paper[23] has reported the phase diagram of Yukawa systems using molecular-dynamics (MD) simulations. While there are some similarities between the simulation aspects of our work and their studies, there are some crucial differences, a few of which are listed here. One of the aims of the present work has been to elucidate the role of interaction potential in determining the freezing parameters. In addition, they have determined the entire phase diagram by looking for the conditions when a given lattice type becomes unstable, i.e., melts. On the other hand, we have primarily been interested in obtaining freezing and melting parameters by looking at both the crystallization and the melting process in the limit of small κa_s. Finally, we have been interested in features of the interaction potential that may be responsible for the occurrence of reentrant melting behavior in these systems.

This paper is organized as follows. In Sec. II we present discussion of the choice of the model interaction potential for charge stabilized colloidal systems. For the range of the screening parameters encountered in this work, the so-called Derjaguin-Landau-Verwey-Overbeek (DLVO) potential is argued to be adequate. A summary of the simulation details is also presented here. Section III discusses the simulation results in detail and the procedure for obtaining the fluid to solid transition is outlined. In Sec. IV the dependence of the results on the system size is discussed. In Sec. V the application of self-consistent phonon theory to determine the global phase diagram is presented. The predictions of this theory are also compared to the MD results. The paper is concluded in Sec. V with a discussion and a few suggestions for an improved theory.

II. MOLECULAR DYNAMICS

A. Interaction potentials

The interaction (electrostatic) potential between the polystyrene spheres suspended in water are well understood and can be readily modeled using the DLVO potential.[25] The DLVO potential is essentially a screened Coulomb interaction and arises as a solution to the linearized Poisson-Boltzmann equation. By adding salt (or other electrolytes) to the system the effective screening can be increased or decreased and this results in the formation of the various phases described in the Introduction. The pairwise DLVO potenial between two particles is given by

$$V(|r_i-r_j|)=\frac{Z^2e^2}{\epsilon|r_i-r_j|}\left[\frac{e^{\kappa a}}{1+\kappa a}\right]^2 e^{-\kappa|r_i-r_j|}, \quad (2.1)$$

where a is the polystyrene radius, ϵ is the dielectric constant of water, and Z is the effective charge on the polyball. In Eq. (1) κ is the inverse screening length and is given by

$$\kappa^2=\frac{Ze^2}{4\pi\epsilon k_BT}(\rho_{ps}+2\rho_{salt}), \quad (2.2)$$

where k_B is the Boltzmann constant, T is the temperature, and ρ_{ps} is the polyball number density and ρ_{salt} is the number density of added (assumed to be monovalent) electrolyte solution. Thus, the solvent (water) appears in the potential in accounting for the dielectric nature of the medium. Since we are interested only in the liquid-solid transition, hydrodynamic interactions provided by the medium are irrelevant. For the purposes of analysis it is convenient to define another parameter, Γ, as

$$\Gamma=V(r_0)/k_BT. \quad (2.3)$$

This is in analogy with the coupling constant Γ_{OCP} defined for the one component Coulomb plasma.[26] The DLVO potential given in Eq. (2.1) is quite accurate at densities such that $\kappa r_0\sim O(1)$ and $\kappa a_s<4$, where the Wigner-Seitz radius r_0 is defined by

$$\tfrac{4}{3}\pi r_0^3=\rho_{ps}^{-1} \quad (2.4a)$$

and a_s^3 is the cube of the radius of average separation defined by

$$a_s^3=\rho_{ps}^{-1}. \quad (2.4b)$$

Several previous studies[2,23] have omitted the "geometric factor," $(e^{\kappa a}/1+\kappa a)^2$, in describing the interaction potential. The resulting model potential without this geometric factor will be referred to as the Yukawa potential. The omission of this factor has negligible consequences when $\kappa a\ll 1$, as is the case in very dilute solutions. It has been noted that if a is not much smaller than r_0 then this factor must be included.[24,27] The inclusion of this factor properly accounts for the fact that screening ions cannot occupy the region where the polystyrene molecule is present. Since $V(|r_i-r_j|=a)/k_BT\gg 1$ for all the densities considered here, the geometric factor mimics the hard-core repulsive potential and thus takes into account that the polyballs are not point particles but have a finite radius. The neglect of the geometric factor has profound consequences on the liquid to solid transition as will be shown below. In fact Shih and Stroud[24] claim that without this factor reentrant melting is predicted while inclusion (which is the more realistic description) eliminates this behavior completely. This is discussed further in Sec. IV. In a recent paper,[28] we have used this model potential to obtain pair correlation functions at several (low) densities which were in excellent agreement with the light scattering measurements of Brown *et al.*[6]

We now comment very briefly on the role of attractive forces. Based on microscopy studies, Ito *et al.*[29] have suggested that weak long-range attractive forces may be responsible for phase separations in these systems at low ionic concentration. However, considerations of asymmetric electrolytes have borne out the validity of the DLVO potential.[30–32] By solving a system of hypernetted-chain (HNC) equations one can obtain the direct correlation function from which an effective potential can be calculated. In the limit of the radius of one of the electrolyte components going to zero, the DLVO potential is recovered. Such theories have also been successful in describing small-angle neutron scatter-

ing results of micellar solutions. Thus we conclude that the modeling of the interaction by Eq. (1) does provide a realistic description of the potential between particles in a colloidal liquid. For volume fractions larger than $\phi \sim 0.2$ one needs to take into account the attractive (weak) forces as well.[1]

The effective charge Z is very difficult to determine experimentally. Alexander *et al.*[33] have shown that the Debye-Hückel limit, invoked to derive the DLVO potential, is valid only if the charge is suitably renormalized. Since our results have direct bearing on the experimental work of Lindsay and Chaikin[9] we have taken $Z = 300$, a value recommended by these authors. However, we wish to emphasize that in our results Z is really an adjustable parameter. The other parameters were also chosen in accord with the experimental system. Specifically, the polyball radius a was taken to be 545 Å, the temperature T is 298 K, the dielectric constant $\epsilon = 78.5$, and the mass of the polystyrene molecule m is 4.3×10^8 amu. In all of the simulations we set $\rho_{\text{salt}} = 0$. For these parameters, molecular-dynamics studies were performed to locate the liquid-to-solid transition density. Several volume fractions, $\phi = \frac{4}{3}\pi\rho a^3$, in the range 0.001–0.200, were considered.

We note that for these parameters, the screening is small, i.e., κa_s is in the range 2.0–4.0; hence these are systems that interact strongly over a very long range. It is interesting to note that it is precisely in this regime where the structural predictions based on integral equations such as hypernetted-chain approximation (HNC) or rescaled mean-spherical approximation (RMSA) are very unreliable.[34–39] Because of the inefficient screening, it is found that the results of computer simulations show strong system size dependence and only for large systems (number of particles exceeding 1000) with long equilibration times do we obtain converged results.

B. Simulation details

In order to determine the coexistence of the liquid and solid phases we have numerically integrated the $6N$ coupled classical equations of motion, with N being the total number of particles in the system. For the problem under consideration this involves determining the density ρ_f at which a liquid freezes reversibly into a solid. In addition, one has to find the density ρ_l when the solid reversibly melts. In a majority of the studies of phase transitions on the computer,[40] the freezing density is determined by looking for the lowest density (or temperature) when the solid spontaneously melts. One of the novel aspects of our work is that we have been able to determine the density where the liquid spontaneously freezes into a solid. This may suggest bounds on the coexistence region. We should emphasize such a determination should be viewed with caution because of finite-size dependence. The only previous study (that we are aware of) where this procedure was investigated is the determination of freezing parameters of the Gaussian core liquid by Stillinger and Weber.[41]

Thus the procedure we use entails studying the thermodynamic branches, namely the solid and the liquid branch. Each of the branches represents a well-equilibrated thermodynamic state. The initial configuration for a given thermodynamic state is taken to be the previous configuration of the well-equilibrated state. The initial configurations for the liquid branch is taken to be a lattice. At low-volume fractions it was found that the lattice spontaneously melted. The density was increased slowly until ρ_f was reached when the liquid spontaneously crystallized. Unlike studies involving simple liquids (like Lennard-Jones fluid), where spontaneous freezing into a lattice is harder to achieve, we found that for all the systems studied here (using the DLVO potential), crystallization always occurred at high enough density. The solid branch is generated by using the last crystallized configuration of the liquid branch and expanding gradually (i.e., the density was decreased) until spontaneous melting is observed. A second solid branch, to be referred to as the lattice branch, was generated using the appropriate lattice as the starting configuration for each thermodynamic state. An important distinguishing aspect of the colloidal particles is that because of the strong interaction between the particles the kinetic energy turns out to be just a very small fraction of the total potential energy. This seems to be the main reason that small system sizes, $N \sim 500$ (which is usually sufficient for phase-transition studies in simple liquids) give unreliable results. The N dependence of the results is discussed in Sec. IV.

All of the simulations were performed with the N particles confined to a cubic box, the dimensions of which are adjusted to obtain the appropriate number density. As usual, periodic boundary conditions were employed to minimize surface effects. For the system, size considered in this work, i.e., $N = 1024$ or 864 particles, the value of the potential at the cutoff distance is $0.001 k_B T$ which is comparable to the value typically used in the simulation of the Lennard-Jones system. Time is quoted in units of

$$\tau = (ma^2/k_B T)^{1/2} \tag{2.5}$$

and the time step of 0.005τ was used in the simulations. This translates into 3.6×10^{-9} sec. The time step used in the present simulations is smaller than that typically found in the simulation of Lennard-Jones systems. Because of the large screening length (especially at low densities) a smaller time step was required in order to achieve energy conservation. The classical equations of motion were integrated using the standard Verlet algorithm and in all cases the total energy was conserved to better than one part in a ten thousandth. In all the simulations equilibration was achieved by aging the system for 3000–10 000 time steps. The thermodynamic quantities were calculated by averaging over at least 1000–3000 steps after equilibration was achieved. In some cases it was necessary to perform averages over 10 000 time steps to obtain results within acceptable error bars. The error bars in our simulations are less than 5%.

III. FLUID-SOLID PHASE TRANSITION

A. Lattice sums

It is expected that the arrangement of particles at $T=0$ is crystalline and consequently it is of interest to evaluate the lattice sum for the different lattice configurations. The difference in the energies between bcc, fcc, and hcp lattices are extremely small and consequently at finite temperatures the entropic contribution becomes significant. However, the lattice sums do provide an indication of the relative stability of different lattices for a given thermodynamic condition.

Lattice sums for the Yukawa potential have been performed before and it is known that for $\kappa a_s > 1.72$ the fcc lattice becomes more stable than the bcc lattice.[42,43] For densities such that as $\kappa a_s < 1.72$ the bcc lattice is found to be more stable. The appropriate lattice sum is evaluated using

$$E=\frac{Z^2e^2}{\epsilon}\left[\frac{e^{\kappa a}}{1+\kappa a}\right]^2\sum_l\frac{\exp[-\kappa x(l)]}{x(l)}\ , \tag{3.1}$$

where $x(l)$ is the modulus of the lattice vector corresponding to a given lattice. For the form of the DLVO potential the summation over l can be calculated using the Ewald method and it is, in fact, necessary to do this when the screening length is large. We have chosen to evaluate the lattice sums directly on the computer, because in the screening region of interest, the sum over l converges rapidly.

The sum in Eq. (5) was evaluated for fcc, bcc, and sc lattice structures The lattice spacing for a given structure is given by

$$l=(c/\rho)^{1/2} \tag{3.2}$$

with $c=1$, 2, and 4, for the sc, bcc, and fcc crystalline arrangement, respectively. For each lattice the sum over l in Eq. (5) was evaluated using about 30 000 lattice sites where E was converged to better than 1 part in 10^5. In Fig. 1 we plot

$$\Delta E=(E_{\rm bcc}-E_{\rm fcc})/k_BT \tag{3.3}$$

as a function of κa_s. It is clear that according to lattice sum calculations, for both the Yukawa potential and for the DLVO potential the fcc lattice is more stable for the range of κa_s of interest in this paper. However, we shall show below that MD results (and experiments) for the DLVO potential clearly show that the bcc phase is the more stable one and as the density of polyballs is increased the liquid freezes into this structure. As stressed earlier this transition is entropically driven and consequently lattice sums alone cannot predict the stability of the crystalline phase.

B. Equation of state

In this section we discuss the compressibility, $Z=PV/Nk_BT$, as a function of the volume fraction for both the DLVO potential and the Yukawa potential. The results have been obtained for $N=864$. In Fig. 2, Z as a function of the volume fraction for the liquid and solid branches of the DLVO potential and for the liquid branch of the Yukawa potential is presented. The two branches for the DLVO potential are superimposable on this scale. As the volume fraction tends to zero (the noninteracting or ideal limit) Z should tend to unity. The compressibility for the DLVO potential is expected to increase monotonically until ϕ reaches a certain value ϕ_m and then Z would decrease as ϕ as increased further. This behavior for Z at $\phi\sim\phi_m$ is inferred by examining the DLVO potential evaluated at $r=\rho^{-1/3}$ as a function of ϕ. For $\phi\sim\phi_m$ the dependence of Z on ϕ is a reflection of the competition between the Coulomb part of the potential and the counterion screening, i.e., the value of q^{-1}. As the volume fraction is increased fur-

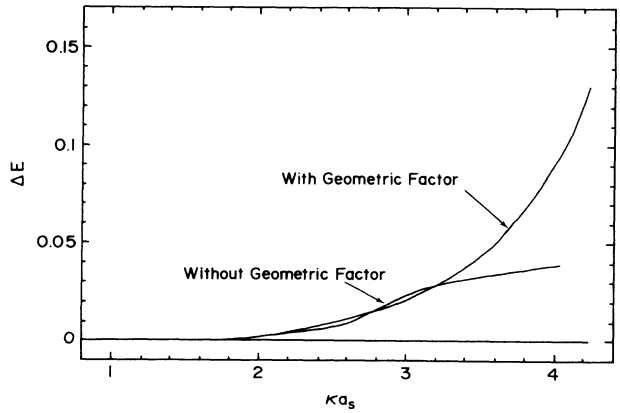

FIG. 1. Lattice energy difference between the bcc and fcc phases, $\Delta E=(E_{\rm bcc}-E_{\rm fcc})/Nk_BT$, as a function of κa_s (essentially the polystyrene density). Both the DLVO system ("with geometric factor") curve and the curve for the Yukawa system ("without the geometric factor") are plotted. At $\kappa a_s=1.72$, both curves fall below 0.0 (not perceptible in the figure) indicating bcc as the stable phase. Above $\kappa a_s=1.72$, both curves show that fcc is the stable phase in contradiction to MD results.

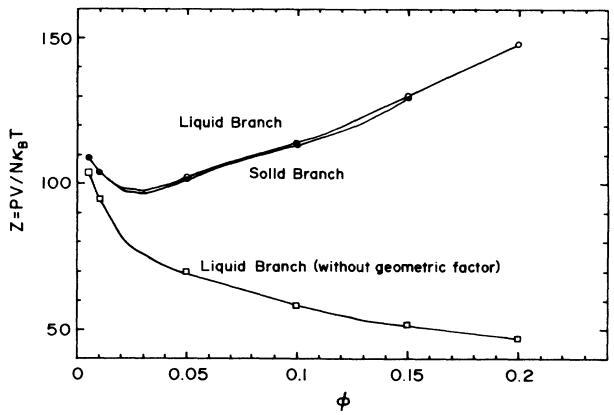

FIG. 2. Equation of state for polystyrene spheres. The compressibility $Z=PV/Nk_BT$ is plotted vs the volume fraction. The upper two curves are the liquid and solid branches for the DLVO system. The lowest curve is the compressibility for the Yukawa system (without the geometric factor).

ther, a minimum in Z is obtained at $\phi=\phi_{\min}$ and for $\phi>\phi_{\min}$, Z monotonically increases. For $\phi\geq\phi_{\min}$ the geometric factor essentially plays the role of hard core and Z behaves as in a simple liquid. On the other hand, the Yukawa potential does not reflect the finite size of the particles and thus for $\phi>0.001$, Z monotonically decreases which is unphysical. Consequently, the particles interacting via the Yukawa potential do not spontaneously freeze into a crystalline configuration and, in fact, there does not appear to be a stable crystalline phase. Over the entire range of volume fractions considered here, the lattice spontaneously melted for the Yukawa system. These considerations lead us to conclude that the pure Yukawa potential does not adequately describe the interaction between particles in an aqueous suspension of polystyrene spheres.

C. Freezing parameters

Molecular-dynamics simulations were used to generate the thermodynamic branches for the liquid and the solid states for the DLVO potential. Each branch clearly exhibits an instability point, i.e., as the density is increased to a critical value ϕ_s, starting from a liquid state the system spontaneously freezes into a bcc phase. Similarly, starting from the solid branch it is found that the system spontaneously melts at a critical low density ϕ_l. This is clearly shown in Fig. 3 where a plot of the thermal fraction of energy $\Delta U/Nk_BT$ as a function of the coupling constant Γ, for each thermodynamic state of $N=1024$ is shown. The thermal fraction of energy is defined as

$$\Delta U/Nk_BT=(U-U_0)/Nk_BT\ , \tag{3.4}$$

where U/N is the potential energy per particle as determined by the MD simulation and U_0 is the corresponding lattice energy. Also shown in this figure is a third curve which is referred to as the lattice curve. Each point on this curve denotes a thermodynamic state where the initial configuration was a perfect bcc lattice. As noted earlier the solid branch is obtained from spontaneous crystallization of the liquid branch and thus the energies of this branch and the lattice curves are expected to coincide for volume fractions greater than 0.15. However, Fig. 3 shows that within error bars, the solid and lattice branches are distinct. This indicates that either the liquid spontaneously crystallizes into a bcc lattice with a few frozen in defects or that the number of particles in the simulation is not adequate. Within the context of the present simulations, these two possibilities cannot be distinguished. Figure 3 indicates that the lattice branch spontaneously melts at $\Gamma=51.3$ ($\phi=0.005$) indicating the instability of the solid while at $\Gamma=167$ ($\phi=0.200$) the liquid spontaneously freezes which is the liquid instability point.

Examination of the pair correlation functions, shown in Fig. 4, for various volume fractions for the liquid branch for $N=864$ demonstrates the dramatic onset of crystallization from the liquid to a bcc lattice at $\phi=0.200$. The peak arrangements in $g(r)$ for $\phi=0.200$ clearly indicate crystallization into a bcc structure. This is in accord with experimental findings. Integration of the pair correlation functions gives the number of nearest neighbors to be 14 for the liquid state. The mean potential energy per particle as a function of the volume fraction for the region $0.001<\phi<0.3$ is found to be well approximated by $14V(2r_0)$. For the Yukawa system, the $g(r)$'s were always liquidlike and remarkably similar over a broad range, $0.001<\phi<0.8$, for both the liquid and lattice branches. We observed no evidence for reentrant melting, in contrast to the predictions of the previous theories.[10,24] It is possible that one has to perform simulations for times much longer than considered here to see evidence for reentrant behavior. However, by considering the crystallization processes exhibited by the DLVO system and using the predictions of the self-consistent phonon theory (see Sec. V) we conclude that reentrant phenomena does not occur in this system. We also note that the results of Kremer

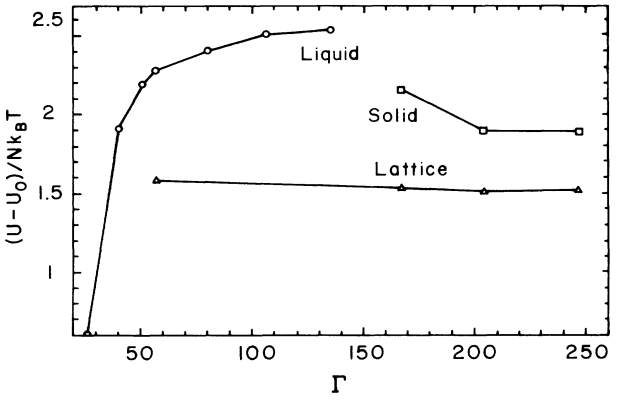

FIG. 3. Thermal fraction of energy, $\Delta U/Nk_BT$, for the three thermodynamic branches as a function of the coupling constant Γ. Thermodynamic points for each branch are connected by a straight line to guide the eye. Maximum in the liquid curve indicates the liquid instability point while the maximum in the lattice curve indicates the solid instability point.

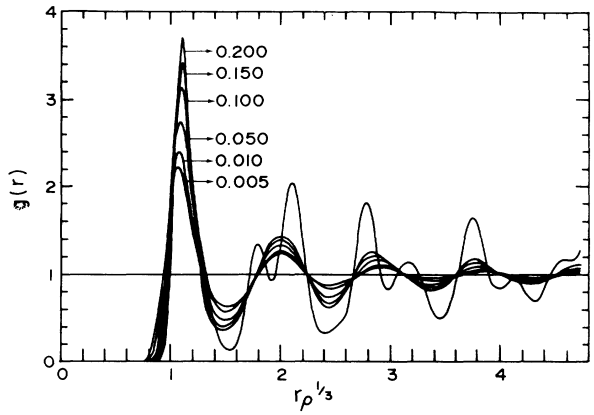

FIG. 4. Pair correlation functions $g(r)$ for $N=864$ as a function of interparticle distances r scaled by the average separation distance $\rho^{-1/3}$. The volume fraction for the various curves is indicated with arrows. For $0.005\leq\phi\leq0.150$, $g(r)$'s are all liquidlike. Top curve is for $\phi=0.200$ and shows peak arrangement consistent with bcc lattice.

et al.,[23] whose simulations cover a larger value of the screening constant κ lend further support to this observation.

There have been several attempts to determine the true transition density from these instability points. In the following we appeal to some of these in determining the order-disorder transition density.

Pollock and Hansen[14] determined the solid instability point for the OCP model and found, through Monte Carlo simulations, that the solid is stable for $\Gamma \geq 139$. Determination of the value of Γ at freezing by equating the free energies of the liquid and solid yielded a value of $\Gamma = 158$ which is about 15% higher than the instability point. If this criteria is applied to the polyball system the melting transition would be predicted to occur at $\Gamma = 65.4$ ($\phi = 0.022$) as compared to the solid instability point of $\Gamma = 56.8$ ($\phi = 0.01$).

Raveche, Mountain, and Street[45] discovered an empirical rule governing the freezing of Lennard-Jones systems based on the examination of the pair correlation function. It was found that when the liquid freezes, the ratio, $\alpha = g(r_{\min})/g(r_{\max})$, where $r_{\max}$ is the distance corresponding to the maximum in the radial distribution function (RDF) and $r_{\min}$ is the distance corresponding to the subsequent minimum in $g(r)$, is approximately 0.2. Invoking this criteria for $N = 864$ and for 1024, we find that the freezing parameters are $\Gamma = 70.2$ ($\phi = 0.027$) and $\Gamma = 63.7$ ($\phi = 0.017$), respectively. These values are in fair agreement with the estimate based on analogy with the OCP results made above.

The Verlet[46] rule which states that at freezing the maximum in the structure factor $S(k_{\max}) \sim 2.85$ is found to hold remarkably for systems interacting with a $1/r^n$ potential. Use of this criterion for the present system yields a value of $\Gamma = 69.5$ ($\phi = 0.026$) and $\Gamma = 68.0$ ($\phi = 0.023$) for the $N = 864$ and 1024 particle systems, respectively.

Finally, we examine the Lindemann criterion which states that the solid should melt when the ratio of the square root of the mean-square distance, $\langle r^2 \rangle^{1/2}$, to the lattice spacing d exceeds 0.1. In the upper panel of Fig. 5 a plot of the radial distribution function, $g(r/r_0)$, as a function of r/r_0 for $\phi = 0.01$ is presented. The initial configuration for this state is a perfect bcc lattice. The RDF shows that this state is crystalline with signatures of bcc phase. In the lower panel, the mean-square displacement (MSD) as function of $\omega_p t$ (with $\omega_p^2 = m/4\pi Z^2 e^2 \rho$) for the same state is presented. This figure shows that MSD has saturated at $R_{\max}$ further indicating that the thermodynamic state is crystalline. We also find that the resultant diffusion coefficient is about 2 orders of magnitude smaller than what is observed in the liquid state. The ratio of $R_{\max}/d$ is found to be 0.23. This indicates that the particles execute very large amplitude motion near melting. Thus, the low-frequency modes dominate near the melting transition and seem to describe the dynamics before the lattice becomes unstable. It is interesting to point out that Kremer, Robbins, and Grest[23] found that the Lindemann parameter for the Yukawa potential was about 0.19. The corresponding value for Lennard-Jones crystals is only about 0.1. The very large value of the Lindemann criteria is the major reason for the failure of the self-consistent phonon theory. This is discussed in Sec. V.

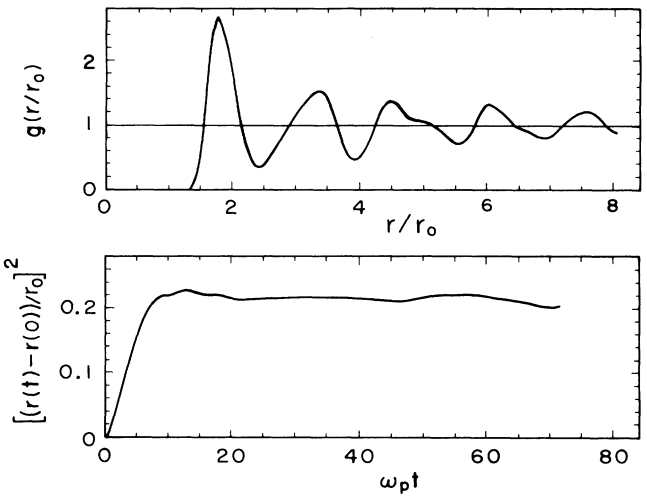

FIG. 5. Lindemann parameter for the $N = 1024$ system. Upper panel shows $g(r)$ as a function of r/r_0, where r is the Wigner-Seitz radius. Structure indicates that the system is still a lattice. Lower panel shows mean-square displacement as a function of time. Here time is scaled by the plasma frequency, ω_p (defined in the text). Saturation of the mean-square displacement of infinite times yields a Lindemann ratio of 23%.

It is clear that all of the empirical criteria lead to reasonably similar results for the density at which freezing takes place. The average value of the density is found to be $\phi = 0.023 \pm 0.004$ which corresponds to $\Gamma = 67 \pm 3$.

IV. SIZE DEPENDENCE OF SIMULATION RESULTS

In the previous section the molecular-dynamics calculations for the fluid-solid transition were presented based on the results obtained with $N = 864$ or 1024 particles. The range of interaction of the model potentials used in our simulations is long and consequently the sensitivity of the results to the system size becomes a crucial question. It should be pointed out that even at the smallest volume fraction considered in this work and with $N = 250$ the value of the potential at the cutoff distance is of the order of $10^{-3} k_B T$. This suggests that Ewald corrections are not needed to achieve accuracy. However, it is known that near the fluid-solid transition large system size is required to yield results close to the thermodynamic limit. It is for this reason that the investigation of the dependence of the results on the system size is important.

We have systematically studied the properties of the system for $N = 250$, 256, 512, 729, 864, and 1024 at various values of ϕ. For purposes of discussion we focus our attention on the results obtained with a few of these systems. For $N < 500$ particles it was found that starting from a liquid and increasing the density leads to solidification at volume fractions smaller than is ob-

tained with larger systems. More importantly, the nature of the crystalline phase is dependent on the initial lattice configuration. For example, a 256-particle system with an initial fcc lattice configuration crystallizes into a fcc phase while a 250-particle system with an initial bcc phase solidifies into a bcc phase. For $N > 500$ particles but less than about 800 particles, the crystallization depends on the way the density of the system is changed. In particular, starting from a liquid configuration, if the density is increased slowly (small increments) spontaneous crystallization is achieved at a density, ϕ^*, which is much smaller than the value obtained with a larger (i.e., $N = 1024$) system. However, if ϕ is increased from a liquidlike state to a value past ϕ^* the system exhibits liquidlike behavior and crystallization takes place only at the higher volume fraction, in agreement with the result obtained with the larger systems. The crystalline phase is a bcc regardless of the path used to reach the state. Only for N greater than 800 does one obtain accurate results, i.e., the density at which spontaneous crystallization takes place is independent of both the starting initial configuration and the way the system density is changed. This is clearly shown in Fig. 6, where the pair correlation function at various values of ϕ for $N = 864$ and 1024 is shown as a function of ra_s^{-1}. For all values of ϕ except $\phi = 0.2$ the results are in perfect agreement. For $\phi = 0.2$, it is clear that both $g(r)$'s resemble that of a bcc lattice but the peak heights of the second neighbors are not identical. Thus for a quantitative determination of the structure one should use at least 1000 particles in the simulation. Clearly for different parameters, i.e., shorter screening distance, one can perhaps obtain reliable results with smaller systems.[23]

The thermal fraction of energy is quite sensitive to N. For N less than 1000 it was found that the $\Delta U/Nk_BT$ exhibited no systematic trend. Only with $N = 1024$ did we find a monotonic increase of $\Delta U/Nk_BT$ with ϕ. This dependence on N was also seen in the simulation of one

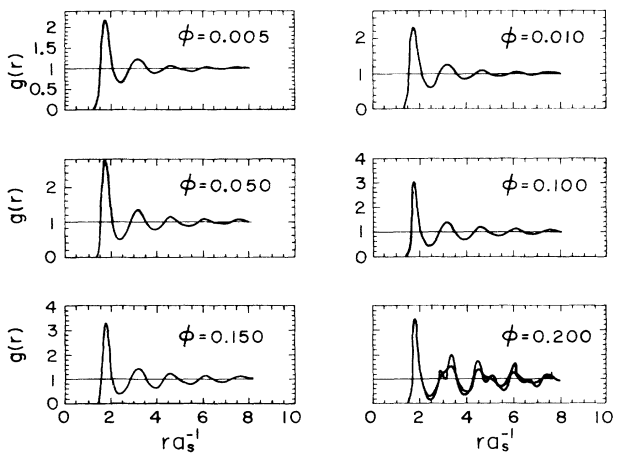

FIG. 6. Pair correlation function $g(r)$ as a function of ra_s^{-1} for various values of the volume fractions. The results are presented for both $N = 864$ and 1024. For all values of ϕ, except for $\phi = 0.200$, the results obtained with both the systems are identical.

component Coulomb plasma.[26] The dependence of the results on N is an indication of the existence of severe bottlenecks in phase space that can apparently be overcome by using a large system size. Thus when N is small the system can get trapped in one of the metastable states and it would require a long time to make a transition to a lower energy state. We believe that the reason for the serious system size dependence is primarily due to the very strong interaction between the particles. This makes it necessary not only to use large systems but also requires lengthy molecular-dynamics runs to obtain results close to the thermodynamic value.

V. SELF-CONSISTENT PHONON THEORY

The molecular-dynamics results presented in Sec. III do not seem to be explained by the theories presented by Shih and Stroud[24] or that of Hone *et al.*[22] Because of the uncertainties in both these theories we have used the self-consistent phonon theory[47,48] using both the Einstein approximation[49] and the Debye approximation to compute the phase diagram of colloidal suspensions. The natural objection to the use of the self-consistent phonon (SCP) theory is that the phase diagram is solely determined by considering the free energy of only the solid side. No information about the behavior of the liquid phase is taken into account. On the other hand, in the much studied density functional theory of freezing[50] (DFT), the free energy of the solid phase is expanded about that of the liquid phase. Reference to the crystal phase is made only in determining the conditions under which the density wave of the solid phase becomes stable. The application of DFT requires the knowledge of direct correlation function $C(r)$ of the liquid phase. For polyballs, it is difficult to calculate $C(r)$ using standard integral equations accurately for high enough volume fractions. However, it can be determined from the present MD simulations and then DFT can be used. This will be pursued elsewhere.[51]

The self-consistent phonon (SCP) theory of melting can be derived in many ways. Following Boccara and Sarma,[47] we derive it using the Gibbs-Bogolyubov inequality. Let the Hamiltonian of the crystal be

$$H = \sum \frac{P_i^2}{2m} + \tfrac{1}{2} \sum_{i,j} V(R_{ij} + u_i - u_j) , \tag{5.1}$$

where $\mathbf{R}_{ij}$'s are vectors joining the equilibrium lattice points at site i and j and u_i and u_j are the dynamical displacement due to thermal vibrations. The essential idea of SCP is to approximate the Hamiltonian by a trial Hamiltonian consisting of a collection of the linear harmonic oscillators in which the spring constants, as well as the thermally averaged displacement-displacement correlation functions are determined variationally. Systematic improvement over this theory using standard diagram techniques can be made although these become increasingly difficult.[52] In the diagrammatic language, the SCP theory includes topological diagrams of the Hartree type.[52] The variationally determined displacement-displacement correlation function can be combined with the Lindemann criteria to determine the

melting transition.

The trial harmonic Hamiltonian is written as

$$H_R=\sum_i \frac{P_i^2}{2m}+\tfrac{1}{2}\sum_{i,j}\tfrac{1}{2}(u_i-u_j)\phi_{ij}(u_i-u_j)\ , \tag{5.2}$$

where the force constants ϕ_{ij} are to be determined variationally. The Gibbs-Bogolyubov inequality states that

$$F\le F_T\equiv F_h+\langle V-V_T\rangle\ , \tag{5.3}$$

where F_T is the trial free energy, F_h is the free energy of the reference harmonic Hamiltonian, V is the total potential energy of the actual system, and V_T is the total potential energy of the reference oscillator system. The trial free energy F_T can be written in the form

$$F_T=\langle H+k_BT\ln\rho_R\rangle\ , \tag{5.4}$$

where the average of f is defined as

$$\langle f\rangle=\mathrm{Tr}(fe^{-H_R/k_BT})/\mathrm{Tr}e^{-H_R/k_BT} \tag{5.5}$$

and k_B is the Boltzmann constant. The harmonic approximation to the free energy F_h is

$$F_h=\langle H_T+k_BT\ln\rho_R\rangle \tag{5.6a}$$

with

$$\rho_R=e^{-H_R/k_BT}/\mathrm{Tr}e^{-H_R/k_BT}\ . \tag{5.6b}$$

Thus the trial free energy F_T, which is the upper bound to the true free energy, becomes

$$F_T=F_h+\tfrac{1}{2}\sum_{i,j}\langle V(R_{ij}+u_i-u_j)\rangle-\tfrac{1}{4}\sum\lambda_{ij}:\phi_{ij}\ , \tag{5.7}$$

where

$$\lambda_{ij}^{\alpha\beta}=\langle(u_i-u_j)_\alpha(u_i-u_j)_\beta\rangle\ . \tag{5.8}$$

Recalling that ∇ is the displacement operator one can write

$$\langle V(R_{ij}+u_i-u_j)\rangle=\langle\exp(u_i-u_j)\nabla\rangle V(R_{ij})$$

which for averages over harmonic reference system becomes $\exp(\frac{1}{2}\lambda_{ij}:\nabla\nabla)V(R_{ij})$. Thus Eq. (5.7) becomes

$$F_T=F_h+\tfrac{1}{2}\sum_{i,j}\exp(\tfrac{1}{2}\lambda_{ij}:\nabla\nabla)V(R_{ij})-\tfrac{1}{4}\sum_{i,j}\lambda_{ij}:\phi_{ij}\ . \tag{5.9}$$

The variational equations are obtained by treating λ_{ij} and ϕ_{ij} as parameters and this gives the following coupled self-consistent equations:

$$\frac{\delta F_h}{\delta\phi_{ij}}-\tfrac{1}{4}\lambda_{ij}=0 \tag{5.10a}$$

and

$$\lambda_{ij}=\langle(u_i-u_j)(u_i-u_j)\rangle\ . \tag{5.10b}$$

The harmonic free energy can be expressed in terms of the frequencies (the eigenvalues) of the dynamical matrix, i.e.,

$$\sum_\beta D_{\alpha\beta}\hat{\epsilon}_\beta(\mathbf{k},j)=\omega_{k\alpha}^2\hat{\epsilon}_\alpha(\mathbf{k},j)\ , \tag{5.11a}$$

where

$$D_{\alpha\beta}(\mathbf{k})=\frac{1}{Nm}\sum_{i,j\ne1}^{N}[1-\exp(-i\mathbf{k}\cdot\mathbf{R}_{ij})]\times\nabla_\alpha\nabla_\beta\langle V(R_{ij}+u_i-u_j)\rangle\ . \tag{5.11b}$$

The vectors $\epsilon_\alpha(kj)$ is the αth component of the unit eigenvector of the jth branch of the mode $\mathbf{k}$. The force-constant matrix in Eq. (5.11b) can be written in the following form which is more useful for practical calculation:

$$\langle V(R_{ij}+u_i-u_j)\rangle=[(2\pi)^3\det\lambda_{ij}]^{-1/2}\times\int d^3u\ V(R_{ij}+u)\exp(\tfrac{1}{2}u\lambda_{ij}^{-1}u)\ . \tag{5.12}$$

The practical implementation involves solving the eigenvalue equation (5.11a) for a trial force-constant matrix and knowing the frequencies and the eigenvectors one can calculate λ_{ij} as

$$\lambda_{ij}^{\alpha\beta}=\frac{1}{N}\sum_{k,s}\frac{[1-\cos(\mathbf{k}\cdot\mathbf{r}_{ij})]}{m\omega_{ks}}\hat{\epsilon}_\alpha(k_s)\hat{\epsilon}_\beta(k_s)\coth(\beta\hbar\omega_{ks}/2)\ . \tag{5.13}$$

Knowing λ_{ij} an improved renormalized potential can be computed using Eq. (5.12) and a new force-constant matrix can be constructed. This process can be repeated until convergence is obtained. The full solution of these self-consistent equations will be presented elsewhere. In order to get an analytically tractable expression, in what follows, we present a simplified treatment, namely, the self-consistent Einstein approximation and the self-consistent Debye approximation.

In the Einstein approximation, the trial Hamiltonian is written as a sum of independent oscillators, i.e.,

$$H_T=\sum_x\frac{P^2}{2m}(x)+\tfrac{1}{2}m\omega^2\sum_x u^2(x)\ , \tag{5.14}$$

where x denotes the lattice site and $u(x)$ is the dynamical displacement associated with that site. Assuming that λ_{ij} is independent of sites and of the component, i.e.,

$$\lambda_{ij}^{\alpha\beta}=\lambda\delta_{\alpha\beta}\ . \tag{5.15}$$

The trial free energy per particle $f_T=F_T/N$ becomes [see Eq. (5.9)]

$$f_T=3k_BT\ln[2\sinh(\beta\hbar\omega/2)]+\tfrac{1}{2}\sum_{\mathbf{x}\,(\ne0)}e^{(1/2)\lambda\nabla^2}V(R_{\mathbf{x}})-\tfrac{3}{4}m\omega^2\lambda\ . \tag{5.16}$$

The first term is the free energy of the reference system, the second term is an approximation to the second term in Eq. (5.7) with the assumption given by Eq. (5.14). For the potential of the form

$$Ae^{-qR_x}/R_x$$

one can calculate the second term in Eq. (5.16) and the trial free energy becomes

$$f_T = 3k_B T \ln[2\sinh(\beta\hbar\omega/2)] + \frac{A}{4} e^{q^2\lambda/2} \sum_{x\,(\neq 0)} \frac{1}{R_x} \{ \mathrm{erf}(q\lambda + R_x)/\sqrt{2\lambda}]e^{qR_x} - \mathrm{erf}[(q\lambda - R_x)/\sqrt{2\lambda}]e^{-qR_x} - 2\sinh(qR_x)\} - \tfrac{3}{4} m\omega^2\lambda \ , \tag{5.17}$$

where erf(x) is the error function. The parameters, namely the Einstein frequency ω and the displacement correlation function λ, are determined by minimizing f_T and this leads to the following self-consistent equations:

$$\lambda = \frac{\hbar \coth(\beta\hbar\omega/2)}{m\omega} \tag{5.18a}$$

and

$$\omega^2 = \frac{A}{3m} e^{q^2\lambda/2} \sum_{x\,(\neq 0)} \left[\frac{q^2}{2} \{ e^{qR_x} \mathrm{erfc}[(q\lambda + R_x)/\sqrt{2\lambda}] - e^{-qR_x} \mathrm{erfc}[(q\lambda - R_x)/\sqrt{2\lambda}] \} - \left[\frac{2}{\pi\lambda^3} \right]^{1/2} \exp[-(q^2\lambda^2 + R_x^2/2\lambda)] \right] , \tag{5.18b}$$

where erfc is the complement of the error function. Equation (5.18a) in the classical limit becomes

$$\lambda = 2/\beta m\omega^2 \ . \tag{5.18c}$$

Notice that Eq. (4.17) correctly reduces to the equations for the classical one component Coulomb plasma when $q = 0$.[48] The parameter λ is related to the mean square displacement by

$$\lambda = \tfrac{2}{3}\langle u^2 \rangle \tag{5.19}$$

and thus knowing λ enables us to calculate the Lindemann parameter.

In order to determine the melting curve and hence the phase diagram one has to obtain the free energy of both the liquid phase as well as the solid phase. Here we simply invoke the Lindemann criteria which states that the solid phase becomes unstable (i.e., melts) when the mean-square displacement exceeds the lattice spacing by a certain amount, i.e.,

$$\frac{\langle u^2 \rangle}{a^2} = c$$

with c being about 0.01. In obtaining the phase diagram several values of c have been used. Two of them, namely, $c = 0.025$ and 0.033, were considered by Hone *et al.*[22] The molecular-dynamics simulation results indicate that $c \approx 0.048$ implying that the charged colloid system tolerates large amplitude motion. We have also used the value of $c = 0.01$. The phase diagram using the self-consistent (Einstein) (SCE) phonon theory is obtained by solving Eqs. (5.18b) and (5.19c). The resulting phase diagram for the various c values is presented by plotting $T_R^{-1} = Z^2 e^2/\epsilon a_s k_B T$ as a function of κa_s. Recall that κ can be changed by adding an electrolyte to the colloidal suspension. The phase diagram is shown in Fig. 7 for various c values quoted above. Because the qualitative results for different c values are the same we will discuss the phase diagram by referring to the curve with $c \approx 0.048$. There are several features of the phase diagram that are worth pointing out: (a) For $T_R \leq 0.095$, the stable solid phase is always bcc as long as κa_s is less than 1.72. As κa_S is increased beyond this value there is a transition between bcc→fcc→ liquid. However, for $T_R > 0.055$ the bcc phase melts directly without the transformation to the intermediate fcc state. (b) The fcc is no longer stable for $T_R > 0.055$, a value considerably larger than the one predicted by Hone *et al.*[22] (c) We find no evidence for reentrant behavior. This is also in contrast to the theory of Hone *et al.*[22] who find that for certain values of T_R a reentrant behavior in which the system undergoes a phase transition from bcc→fcc→bcc. (d) For large T_R the range of κa_s over which the fcc is stable decreases. (e) The pre-

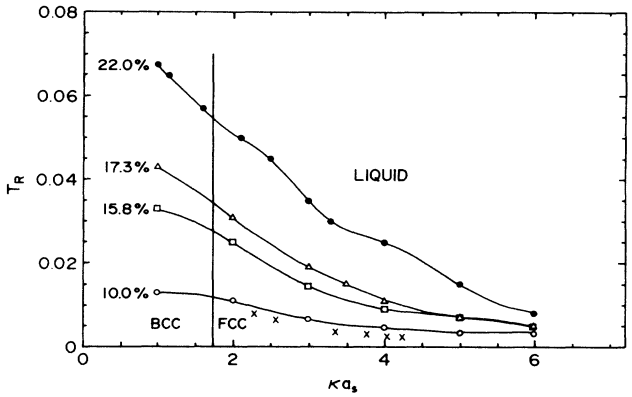

FIG. 7. SCE phase diagram as a function of the renormalized temperature T_R (see text) and the screening κa_s. Three thermodynamic states are shown, bcc solid, fcc solid, and liquid. bcc is stable for $\kappa a_s < 1.72$ and fcc is stable for $\kappa a_s > 1.72$ as indicated by the solid vertical line. Various Lindemann curves indicate the region where the liquid is stable. Four Lindemann curves are shown; 10% is the standard Lindemann ratio, $c^{1/2}$; above this curve the liquid is stable. $c^{1/2} = 15.8\%$ to 17.3% indicates the Lindemann range valid for hard sphere. The top curve has $c^{1/2} = 22\%$, a value consistent with MD results. Diagram shows no reentrant melting nor any reentrant bcc phase behavior. The crosses are the thermodynamic states used in the simulations.

dictions of the SCE are in complete disagreement with both the experimental studies as well as the molecular-dynamics results. The MD results are shown as crosses in Fig. 7. Computer simulation studies reported in Sec. III and experiments predict that for $T=300$ K the liquid freezes into a bcc phase. The reason for this may be because this system is much more anharmonic than the OCP. Furthermore the SCE theory does not account for the dispersion in the frequency and this approximated by a single frequency.

Given the failure of the SCE model, we look towards the next level of approximation. Here we include the dispersion in the frequency, a feature ignored by the SCE model, by solving the full set of dynamical equations, given by Eqs. (5.10) and (5.11). The frequencies are then obtained as the eigenvalues of the dynamical matrix corresponding to the renormalized potential, Eq. (5.10). The displacement parameter λ is given by

$$\lambda=\frac{1}{3N}\sum_i 2/\beta\omega_i^2 m \ , \tag{5.20}$$

where $3N$ is the number of normal modes. The free energy of the bcc lattice for $\phi=0.005$, $N=1024$ was calculated. The resulting free energy and Lindemann parameter, $c^{1/2}$, are in good agreement with the SCE results.

Thus the failure of the SCE model does not appear to lie in the neglect of the dispersion in frequency. However, we note that the $c^{1/2}$ values from SCE would predict a melting transition at $\phi=0.003$, if $c^{1/2}=10\%$. If we choose $c^{1/2}=22\%$, the predicted melting transition is several orders of magnitude smaller than the MD result of $\phi=0.023$. Thus the SCE Lindemann parameters are too small. Since the Lindemann parameter is inversely proportional to the sum of the frequencies squared, we suspect that SCE ignores the low-frequency motions. The MD results show that large amplitude motions are important near melting. We may conclude that the failure of SCE and other lattice dynamical theories is due to the neglect of low-frequency modes, prevalent near melting. This feature does not appear important for melting of Ar[47] where the SCP theory is found to be successful. However, when the Lindemann parameter is large, theories based on harmonic treatment cannot be successful in predicting accurate melting temperatures.

VI. CONCLUSIONS

In this paper we have presented simulations as well as a simple theoretical application of the self-consistent phonon theory to study disorder-order transition in aqueous suspension of charged polystyrene spheres. We conclude this paper with a summary of our observations and a few additional comments.

(a) The molecular-dynamics results were used to locate the densities at which spontaneous crystallization ($\phi=\phi_s$) at which the solid becomes unstable ($\phi=\phi_m$). By using several empirical criteria the volume fraction at which freezing takes place was found to be $\phi=0.023\pm0.004$. The system is frozen into a bcc lattice and this is clearly reflected in the radial distribution function. It is also shown that close to the lattice instability point, the particles undergo very large amplitude motion. This is reflected in the large value of the Lindemann parameter. The simulation results also indicate that there is no evidence for reentrant behavior in contrast to earlier predictions by some authors.[22,24] The molecular-dynamics results are in agreement with experiments, suggesting that the DVLO potential can describe charge stabilized colloidal suspensions.

(b) Because of the very strong interaction between particles it was found that one has to use sufficiently large number of particles and large number of time steps to obtain results close to the thermodynamic value. This is in contrast to earlier work on OCP where it was shown that using 250 particles (with proper treatment of image charges using Ewald summation technique) one can obtain fairly accurate freezing parameters.[26,44] Our studies show that at least 1000 particles are required to obtain reliable results. However, when the screening becomes more efficient one can presumably use smaller system sizes.[23]

(c) The phase diagram calculated using the self-consistent phonon theory does not appear successful in the weak screening limit. The theory predicts that for the thermodynamic condition considered in this article the crystalline phase is fcc which is disagreement with both the simulation and the experiment. However, it successfully predicts that there is no reentrant melting (or freezing) which is in accord with the simulation results.

(d) We have attempted to use the results of the density functional theory by using the hard sphere as a reference system.[24,53] Using Gibbs-Bogolyubov inequality, the optimum value of the hard-sphere packing η can be obtained. With this one can use density functional theory of freezing to obtain the density at which freezing occurs. The transition density was found[51] to be six times larger than that predicted by simulations. Moreover, this theory is found to be extremely sensitive to the value of Z used.[51]

(e) After this paper was completed we became aware of a very recent paper[54] in which few formulas for the self-consistent phonon theory presented in Sec. V have been derived. These authors used the hard-sphere reference system to calculate the liquid free energy.[51] From these the phase diagram for the colloidal suspension was obtained. The interested should certainly refer to this work.

Note added in proof. After submitting this paper, we have obtained the phase diagram (analogous to that given in Fig. 7) by assuming a Debye spectrum for the oscillators. The appropriate free energy, in the classical limit, for the case is found to be

$$f_T=3kT(\ln\beta\hbar\omega_D-\tfrac{1}{3})+\tfrac{1}{2}V(\lambda)-\tfrac{9}{4}\lambda m\omega_D^2 \ ,$$

where $\frac{1}{2}V(\lambda)$ is given by the second term in Eq. (5.17). The resulting self-consistent equations are

$$\lambda = \frac{2}{3\beta m \omega_D^2} ,$$

$$\omega_D^2 = \frac{2}{9m} \frac{\partial}{\partial \lambda} V(\lambda) .$$

The resulting phase diagram is identical to that obtained using the Einstein approximation and shown in Fig. 7. This further confirms the conclusion drawn at the end of Sec. IV.

ACKNOWLEDGMENTS

This work was supported by the National Science Foundation under Grant No. CHE-86-09722, the Camille and Henry Dreyfus Foundation, the Alfred P. Sloan Foundation, and the Presidential Young Investigators Program. In addition, acknowledgment is made to the Donors of the Petroleum Research Fund, administered by the American Chemical Society, for partial support of this research.

[1]P. Pieranski, Contemp. Phys. **24**, 25 (1983).

[2]W. Van Megen and I. Snook, Adv. Colloid Interface Sci. **21**, 119 (1984).

[3]C. S. Hirtzel and R. Rajagopalan, *Colloidal Phenomena Advanced Topics* (Noyes, Park Ridge, NJ, 1985).

[4]J. B. Hayter, Physica B&C **136**, 269 (1986).

[5]D. W. Schaefer, J. Chem. Phys. **66**, 3980 (1977).

[6]J. C. Brown, P. N. Pusey, J. W. Goodwin, and R. H. Ottewill, J. Phys. A **8**, 664 (1975); F. Gruner and W. P. Lehmad, *ibid.* **15**, 2487 (1982).

[7]The possibility of ordering in these systems was anticipated by J. G. Kirkwood and J. Mazur, J. Polym. Sci. **9**, 519 (1952).

[8]R. Williams and R. S. Crandall, Phys. Lett. A **48**, 225 (1974).

[9]H. M. Lindsay and P. M. Chaikin, J. Chem. Phys. **76**, 3774 (1982).

[10]P. M. Chaikin, P. Pincus, S. Alexander, and D. Hone, J. Colloid Interface Sci. **89**, 555 (1982).

[11]B. J. Ackerson and N. Clark, Physica A **118**, 221 (1983).

[12]D. Hone, J. Phys. (Paris) Colloq. **46**, C3-21 (1985).

[13]S. Marcelga, D. J. Mitchell, and B. W. Ninham, Chem. Phys. Lett. **43**, 373 (1976).

[14]M. J. Grimson, J. Chem. Phys. **79**, 5070 (1983).

[15]I. K. Snook and W. Van Megan, J. Colloid Interface Sci. **102**, 446 (1984).

[16]A. Kose and S. Hachisu, J. Colloid Interface Sci. **46**, 460 (1974); S. Hachisu and Kobayashi, *ibid.* **46**, 970 (1974).

[17]A. Vrij, F. A. Niewenhuis, H. M. Fijnant, and W. G. M. Agterof, Phys. Lett. A **48**, 225 (1974).

[18]S. L. Brenner, J. Phys. Chem. **80**, 1473 (1976).

[19]H. Fugita and K. Ametani, Jpn. J. Appl. Phys. **16**, 1091 (1977).

[20]D. J. Cebula, J. W. Goodwin, G. C. Jeffrey, R. H. Ottewill, A. Parentich, and R. A. Richardson, Faraday Discuss. Chem. Soc. **76**, 37 (1983).

[21]A. G. Muddle, J. S. Higgins, P. G. Cummins, E. J. Staples, and I. G. Lyle, Faraday Discuss. Chem. Soc. **76**, 77 (1983).

[22]D. Hone, S. Alexander, P. M. Chaikin, and P. Pincus, J. Chem. Phys. **79**, 1474 (1983).

[23]K. Kremer, M. O. Robbins, and G. S. Grest, Phys. Rev. Lett. **57**, 2694 (1986).

[24]W. H. Shih and D. Stroud, J. Chem. Phys. **79**, 6254 (1982).

[25]E. J. W. Verwey and J. G. Overbeek, *Theory of the Stability of Lyophobic Colloids* (Elsevier, Amsterdam, 1948).

[26]J. P. Hansen, Phys. Rev. A **8**, 3096 (1973).

[27]J. O. M. Bockris and A. K. N. Reddy, *Modern Electrochemistry* (Plenum, New York, 1970), Vol. I, Chap. 3.

[28]R. O. Rosenberg and D. Thirumalai, Phys. Rev. A **33**, 4473 (1986).

[29]K. Ito, A. Nakamura, and N. Ise, J. Chem. Phys. **85**, 6136 (1986).

[30]B. Beresford-Smith, D. Y. C. Chen, and D. J. Mitchell, J. Colloid Interface Sci. **105**, 216 (1985).

[31]L. Belloni, Chem. Phys. **99**, 43 (1985).

[32]D. Bratko, H. L. Friedman, and E. C. Zhong, J. Chem. Phys. **85**, 377 (1986).

[33]S. Alexander, P. M. Chaikin, P. Grant, G. J. Morales, and P. Pincus, J. Chem. Phys. **80**, 5776 (1984).

[34]R. P. Keavey and P. Richmond, J. Chem. Soc. Faraday Trans. 2, **72**, 773 (1976).

[35]J. P. Hansen and J. B. Hayter, Mol. Phys. **46**, 651 (1982).

[36]C. A. Castillo, R. Rajagopalan, and C. S. Hirtzel, Rev. Chem. Eng. **1** (1984).

[37]J. Bunce, J. D. F. Ramsay, and J. Penfold, J. Chem. Soc. Faraday Trans. 1, **81**, 2845 (1985).

[38]I. Markovic and R. H. Ottewill, Colloid Polym. Sci. **264**, 454 (1986).

[39]S. H. Chen, Annu. Rev. Phys. Chem. **37**, 391 (1986).

[40]For a review see D. Frankel and J. McTague, Annu. Rev. Phys. Chem. **31**, 491 (1980).

[41]F. H. Stillinger and T. A. Weber, J. Chem. Phys. **68**, 3837 (1978).

[42]J. M. Silva and B. J. Mokrass, Phys. Rev. B **21**, 2972 (1980).

[43]M. Inoue and M. Wadati, J. Phys. Soc. Jpn. **50**, 1027 (1981).

[44]E. L. Pollock and J. P. Hansen, Phys. Rev. A **8**, 3110 (1973).

[45]H. Raveche, R. D. Mountain, and W. B. Street, J. Chem. Phys. **61**, 1970 (1974); H. R. Wendt and F. F. Abraham, Phys. Rev. Lett. **41**, 1244 (1978).

[46]J. P. Hansen and L. Verlet, Phys. Rev. **184**, 141 (1969).

[47]N. Boccara and G. Sarma, Physics **1**, 219 (1969); N. S. Gillis, N. R. Werthamer, and T. R. Koehler, Phys. Rev. **165**, 951 (1968).

[48]For applications of self-consistent-phonon theory to OCP problem, see A. A. Kugler, Ann. Phys. (N.Y.) **53**, 133 (1969); H. Fukuyama and P. M. Platzmann, Solid State Commun. **15**, 677 (1974); H. R. Glyde and G. H. Keech, Ann. Phys. (N.Y.) **127**, 330 (1980); R. C. Albers and J. E. Grubernatis, Phys. Rev. B **23**, 2782 (1981); **33**, 5180 (1986).

[49]Hone *et al.* (Ref. 22) used a truncated form for the potential and used the Einstein oscillator approximation to obtain the phase diagram. The results obtained here, which uses no truncation, are qualitatively different from those obtained in Ref. 22. See also the footnote in Ref. 23.

[50]T. V. Ramakrishnan and M. Yussoff, Phys. Rev. B **19**, 2775 (1979).

[51]D. Thirumalai and R. O. Rosenberg (unpublished).

[52]P. F. Choquard, *The Anharmonic Crystal* (Benjamin, New York, 1967).

[53]B. Firey and N. W. Ashcroft, Phys. Rev. A **15**, 2072 (1977).

[54]W. Y. Shih, I. A. Aksay, and R. Kikuchi, J. Chem. Phys. **86**, 5127 (1987).